https://doi.org/10.15407/ujpe69.8.528

V.M. LOKTEV,[1] V. TURKOWSKI[2]

[1] Bogolyubov Institute for Theoretical Physics, Nat. Acad. of Sci. of Ukraine
*(14-b, Metrologichna Str., Kyiv 03143, Ukraine; e-mail: vloktev@bitp.kiev.ua)*
[2] Department of Physics, University of Central Florida
*(Orlando, FL 32816, USA)*

# SYMMETRY AND VALUE OF THE ORDER PARAMETER IN 2D NEMATIC SUPERCONDUCTORS

*We derive equations for the superconducting nematic order parameter and chemical potential for the hexagonal lattice by accounting for nearest- and next-nearest-neighbor hoppings of electrons. By analyzing the energy of the superconducting ground state, we have found that the symmetry of the order parameter and some other superconducting properties of the system strongly depend on the sign and the magnitude of the next-nearest neighbor hopping. As we will demonstrate, both extended s- and d-pairings significantly contribute to the pairing in the system, that be tuned by changing the hopping parameters. We discuss a possible connection of the obtained results to the properties of several doped monolayer superconductors – graphene and transition metal dichalcogenides.*

*K e y w o r d s*: theory of superconductivity, 2D systems, nematicity.

## 1. Introduction

The possibility of superconductivity in low-dimensional (1D or 2D) physically and technologically important "relativistic" systems, like graphene, recently became a hot topic of research [1–12]. This interest experienced a further jump with discovery of superconductivity in twisted bi-layer graphene, where, as it was shown, at certain twist angles the system demonstrates pronounced superconducting features (for a review, see Ref. [13]). As it was proposed by several authors, the dominating mechanism of pairing in the twisted graphene is the pairing in the nematic channel, where electrons predominantly attract themselves when they occupy nearest sites in different sublattices and are separated by vector that can be defined as the "director" one, i.e., tending to form pairs with a preferable in space orientation.

Currently, the relation between the symmetry of the crystal structure and ***symmetry of the superconducting order parameter*** is a topic of intense debate. The 2D systems with hexagonal, or its particular case – honeycomb, lattices are among the most studied (see, for example, works [7, 14–17]), due to experimental realization of such systems (e.g., graphene, $MoS_2$, *etc.*) that show a potential or demonstrate superconductivity with doping. In particular, in Ref. [7], the mounting theoretical evidences for the existence of a chiral $d$-wave superconducting state in graphene are reviewed, where it is argued that the appearance of the chiral $d$-wave superconductivity in graphene is intimately linked to the hexagonal crystal lattice. In a related study [14], a theoretically-found mixed chirality $d$-wave superconducting state (with topological chiral $d+$ $id$-wave symmetry in one Dirac valley, and $d-$ $id$-wave symmetry in the other one) in the coexistence region between antiferromagnetic (AFM) and superconducting states in lightly doped honeycomb materials was reported.

Dynamical Mean–Field Theory analysis of the extended Hubbard model (with on-site $U$ and nearest-neighbor ($NN$) $V$ interactions) of graphene showed [15] that, at small $U$ and $V$ or a small doping, the system prefers the pairing with the real (nonchiral) triplet $p$-wave symmetry favored for small $V$, while, at large $U$ and $V$ or a small doping, the system is in superconducting regime with the chiral order pa-

Citation: Loktev V.M., Turkowski V. Symmetry and value of the order parameter in 2d nematic superconductors. *Ukr. J. Phys.* **69**, No. 8, 528 (2024). https://doi.org/10.15407/ujpe69.8.528.

rameter combination $p + ip$. Importantly, it was also found that the singlet superconductivity (extended $s$-wave or $d$-wave) is either absent or non-dominant. For another related system – monolayer $MoS_2$ – it was found theoretically [16] that, at a low doping, the odd-parity pairing with $f$-wave Mo $NN$ structure is dominating. Near the van Hove singularity filling, the system favors a ferromagnetic (FM) state, and it was shown that, near this filling, the triplet pairing is driven by FM fluctuations. On the other hand, for a model of correlated doped quantum spin-Hall insulators on honeycomb lattice without inversion symmetry, it was found [17] that, for some range of the parameters, the superconductivity with co-existing spin-singlet $d+id$ and spin-triplet $p+ip$-wave pairing takes place. Thus, hexagonal structures can demonstrate the variety of symmetries of the superconducting pairing.

The type of the model is very important in this sense, in particular, the effect of ***next-nearest-neighbor (NNN) hopping*** can play a rather important, or even a dominant role [18–29]. Thus, in work [20], it was found that, on honeycomb-lattice Hubbard lattice with spin- and charge-fluctuation mediated superconductivity at doping levels of 0.02–0.2 and only local repulsion $U$, a spin-singlet $d_{x^2-y^2} + id_{xy}$-wave pairing is dominating (similarly, the $d$-wave pairing at a low doping was found in work [21]). In this case, the gap is a mixture of the $NN$ and $NNN$ pairings. By moving the offset of the energy level between the two sublattices above the critical value, the authors found the spin-triplet $f$-wave pairing that mainly consists of the $NNN$ pairing. Moreover, it was found that the $NNN$ Coulomb interaction $V$ is also in favor of the spin-triplet $f$-wave pairing. In Ref. [23], it was demonstrated for the Hubbard model on honeycomb lattice that the second- and third-$NN$ hopping amplitudes have a strong effect on the $d+id$-wave pairing symmetry. In a related study [24], it was argued that, in many lattices, the $NN$ and $NNN$ pairings do not spontaneously mix with each other due to the lattice symmetry restrictions, while the honeycomb lattice, due to its uniqueness, provides a possibility to analyze the mixture of the $NN$ and $NNN$ pairing components (in this work, a mixing of different $d$-components was analyzed). In Ref. [25], an analysis of the pairing in doped $MoS_2$ showed a spin-triplet pairing, with $f$-wave pairing for a wide range of doping.

Going beyond hexagonal structures, it was demonstrated for the square lattice and Kagome (modeling system $AV_3Sb_5$) lattice model [26] that there are strong evidences of competing instabilities at higher-order van Hove filling with an $SU(N_f)$ flavor degeneracy ($N_f$ is a number of flavors/types of fermions). In this work, it was found that systems demonstrate rich phase diagrams with FM, AFM superconducting and Pomeranchuk orders. In theoretical studies of other systems, like topological superconductor with hexagonal structure $Cu_xBi_2Se_3$, signs of nematic superconductivity were found [27,28], while, for hole-doped triangular lattice, in the Hubbard model of tin atoms on a silicon substrate it was found [29] that an extended Hubbard interaction is crucial to yield the triplet pairing ($f$-wave ($p$-wave) for moderate (higher) hole doping).

There are also ***experimental*** evidences of a possibility of the chiral superconductivity in highly doped graphene [30]. Namely, at a high doping, when the van Hove singularity in the $\pi$ band is occupied the system can move to an exotic ground state as a result of the many-body interactions. It was shown in Ref. [30] that, with a doping, graphene can be driven through the Lifshitz transition, where the Fermi surface topology evolves from two electron pockets into one large hole pocket.

Below, a possibility of a ground-state nematic superconductivity in a 2D system with honeycomb lattice will be analyzed, paying a special attention to the role of the $NNN$ hopping in the symmetry of the possible order parameters. We will show that the pairing channel in this system is very sensitive to the sign and the magnitude of this parameter, and, therefore, systems with the same lattice structure can show different symmetries of the superconducting state, depending on the tight-binding parameters.

We dedicate this work to $115^{\text{th}}$ anniversary of an outstanding theoretical physicists, one of the founders of the theory of superconductivity, Mykola Bogolyubov. It is well known that, in his works, he considered a Cooper pairing with an isotropic order parameter, without focus on the origin of the attraction between two charge carriers (two electrons or two holes). Our goal in this work is an analysis of the local anisotropic pairing that, in the simplest case, corresponds to a pairing of particles on the $NN$ sites. Such pairs can be regarded as "nematic" elements that, in general,

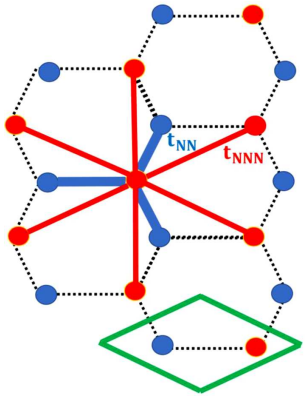


***Fig. 1.*** Crystal structure and unit cells (green) of the honeycomb lattice. The $NN$ and $NNN$ bonds are shown in blue and red, correspondingly

can generate superconducting condensate with both isotropic and anisotropic global order parameters.

## 2. Hamiltonian

The honelycomb lattice and included $NN$ and $NNN$ hopping processes in the system are shown in Fig. 1. The tight-binding Hamiltonian of the system in the case of the $NN$ and $NNN$ hoppings and $NN$ attraction with singlet pairing can be written in the following form:

$$H = -t_{NN} \sum_{\langle \mathbf{n},\mathbf{m}\rangle,\sigma} \left(a^+_{\mathbf{n}\sigma} b_{\mathbf{m}\sigma} + b^+_{\mathbf{m}\sigma} a_{\mathbf{n}\sigma}\right) -$$
$$- t_{NNN} \sum_{\langle\langle \mathbf{n},\mathbf{m}\rangle\rangle,\sigma} \left(a^+_{\mathbf{n}\sigma} a_{\mathbf{m}\sigma} + b^+_{\mathbf{n}\sigma} b_{\mathbf{m}\sigma} + \text{h.c.}\right) +$$
$$+ \mu \sum_{\mathbf{n},\sigma} \left(a^+_{\mathbf{n}\sigma} a_{\mathbf{n}\sigma} + b^+_{\mathbf{n}\sigma} b_{\mathbf{n}\sigma}\right) - V_{\text{attr}} \sum_{\langle \mathbf{n},\mathbf{m}\rangle} \hat{\Delta}^+_{\mathbf{nm}} \hat{\Delta}_{\mathbf{nm}}, \quad (1)$$

where $t_{NN}$ and $t_{NNN}$ are the $NN$ and $NNN$ hoppings (see Fig. 1), and $V_{\text{attr}}$ is the $NN$ attraction. The operator

$$\hat{\Delta}^+_{\mathbf{nm}} = \hat{\Delta}^+_{\mathbf{n},\mathbf{n}+\boldsymbol{\rho}} \equiv \frac{1}{\sqrt{2}} \left(a^+_{\mathbf{n}\uparrow} b^+_{\mathbf{m}\downarrow} - a^+_{\mathbf{n}\downarrow} b^+_{\mathbf{m}\uparrow}\right). \quad (2)$$

in Eq. (1) is the $NN$ spin-singlet creation operator of the superconducting pairs, where $\boldsymbol{\rho}$ are $NN$ vectors. The choice of $NN$ attraction was made for the following reasons. When two electrons with the same spin occupy nearest sites, one of them cannot hope to the neighboring site due to the Pauli principle, thus, there is no effective attraction between them. On the other hand, when one electron has opposite spin to the other, it can hope on the occupied site and then move back (due to Coulomb on-site repulsion with energy $U$) that reduces the pair energy by the order of the exchange constant value $t^2_{NN}/U$ and results in the $NN$ electron-electron attraction, in some sense phenomenologically included into Hamiltonian (1). In fact, the last term in Eq. (1) is similar to the resonance valence bond (RVB) interaction with $V_{\text{attr}} \sim J_{\text{exch}} \sim t^2_{NN}/U$. In this way, we indirectly adopt that, in the system, if it can be described by an effective Hubbard model, the inequality $t_{NN} \ll U$ that excludes double occupancy of the sites is satisfied (the case $t_{NN} \sim U$ requires a separate study).

In order to use the mean-field approximation, let us introduce, as it was done by Bogolyubov, the average of the superconducting the order parameter operator $\hat{\Delta}_{\mathbf{nm}}$:

$$\Delta_{\mathbf{nm}} = \frac{1}{\sqrt{2}} \left(\langle a_{\mathbf{n}\downarrow} b_{\mathbf{m}\uparrow}\rangle - \langle a_{\mathbf{n}\uparrow} b_{\mathbf{m}\downarrow}\rangle\right). \quad (3)$$

Then, in the momentum representation, Hamiltonian (1) becomes

$$H = -t_{NN} \sum_{\mathbf{k},\alpha,\sigma} \left(e^{i\mathbf{k}\boldsymbol{\rho}_\alpha} a^+_{\mathbf{k}\sigma} b_{\mathbf{k}\sigma} + \text{h.c.}\right) -$$
$$- t_{NNN} \sum_{\mathbf{k},\beta,\sigma} \left(e^{i\mathbf{k}\boldsymbol{\rho}'_\beta} a^+_{\mathbf{k}\sigma} a_{\mathbf{k}\sigma} + e^{i\mathbf{k}\boldsymbol{\rho}'_\beta} b^+_{\mathbf{k}\sigma} b_{\mathbf{k}\sigma} + \text{h.c.}\right) +$$
$$+ \mu \sum_{\mathbf{k},\sigma} \left(a^+_{\mathbf{k}\sigma} a_{\mathbf{k}\sigma} + b^+_{\mathbf{k}\sigma} b_{\mathbf{k}\sigma}\right) -$$
$$- \sum_{\mathbf{k},\alpha} \left[\Delta_\alpha e^{i\mathbf{k}\boldsymbol{\rho}_\alpha} \left(a^+_{\mathbf{k}\uparrow} b^+_{-\mathbf{k}\downarrow} + a^+_{\mathbf{k}\downarrow} b^+_{-\mathbf{k}\uparrow}\right) + \text{h.c.}\right] +$$
$$+ 2\frac{N}{V_{\text{attr}}} \sum_\alpha |\Delta_\alpha|^2, \quad (4)$$

where $N$ is the number of $k$-points in the Brillouin zone (BZ), $\boldsymbol{\rho}_\alpha$ ($\alpha = 1,2,3$) are $NN$ vectors, $\boldsymbol{\rho}'_\beta$ ($\beta = 1,...,6$) are $NNN$ vectors and

$$\Delta_\alpha = \Delta_{\mathbf{n},\mathbf{n}+\boldsymbol{\rho}_\alpha} \quad (5)$$

are three 2D space-different order parameters (it is assumed that the system is translationally invariant, so, the order parameters do not depend on the explicit site number $\mathbf{n}$ on the sublattice).

In order to diagonalize the kinetic energy part of Hamiltonian (4), we make the following transformation of the fermionic operators:

$$\begin{pmatrix} a_{\mathbf{k}\sigma} \\ b_{\mathbf{k}\sigma} \end{pmatrix} = \frac{1}{\sqrt{2}} \begin{pmatrix} c_{\mathbf{k}\sigma} + d_{\mathbf{k}\sigma} \\ e^{-i\varphi_{\mathbf{k}}} \left(c_{\mathbf{k}\sigma} - d_{\mathbf{k}\sigma}\right) \end{pmatrix}, \quad (6)$$

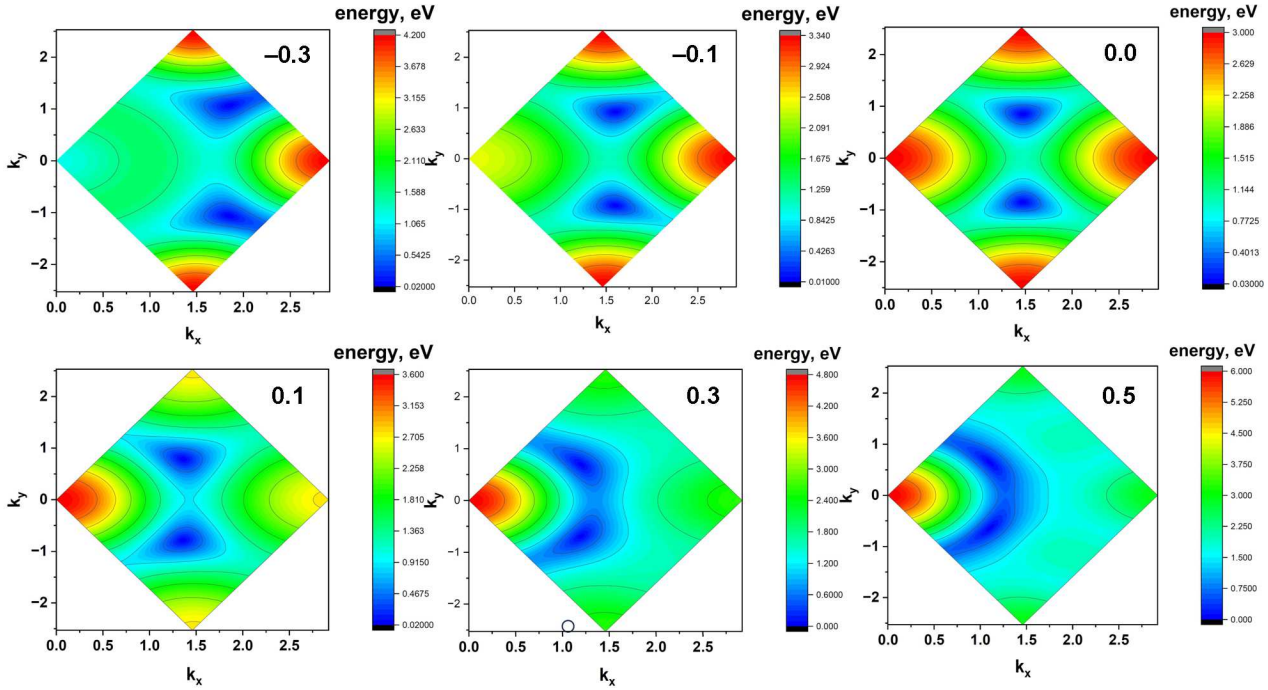


***Fig. 2.*** Band dispersion (7) at $t_{NN} = 1$ eV and different values of $t_{NNN}$ (in eV). The momenta are given in units $2\pi/3a$, where a is the lattice parameter

where $c_{\mathbf{k}\sigma}$ is the annihilation operator in the lower band with energy $(-\varepsilon(\mathbf{k}) + \mu)$, $d_{\mathbf{k}\sigma}$ is the annihilation operator in the upper band with energy $(\varepsilon(\mathbf{k}) + \mu)$. The corresponding bands dispersion is

$$\varepsilon(\mathbf{k}) = \left| t_{NN} \sum_{\alpha} e^{i\mathbf{k}\boldsymbol{\rho}_{\alpha}} + t_{NNN} \sum_{\beta} e^{i\mathbf{k}\boldsymbol{\rho}'_{\beta}} \right|. \tag{7}$$

Spectrum (7) at different values of the $NNN$ hopping is shown in Fig. 2. As it follows from this figure, when there is no NNN hopping, the minimum of the spectrum is in $\mathbf{K}$ and $\mathbf{K}'$ (Dirac) points (blue minima in the bottom figure of the central column). With increase of the modulus of the $NNN$ hopping, the minima of the energy shift form the center of the BZ and become elongated forming Fermi pockets of similar form, most extended at large positive $t_{NNN}(=0.5$ eV).

In Eq. (6),

$$\varphi_{\mathbf{k}} = \arg\left( t_{NN} \sum_{\alpha} e^{i\mathbf{k}\boldsymbol{\rho}_{\alpha}} \right) \tag{8}$$

is the angle of the complex number $t_{NN} \sum_{\alpha} e^{i\mathbf{k}\boldsymbol{\rho}_{\alpha}}$ with respect to the real axis.

In new operators, Hamiltonian (4) acquires the form

$$H = -\sum_{\mathbf{k},\sigma} \varepsilon(\mathbf{k})\, c^{+}_{\mathbf{k}\sigma} c_{\mathbf{k}\sigma} + \sum_{\mathbf{k},\sigma} \varepsilon(\mathbf{k})\, d^{+}_{\mathbf{k}\sigma} d_{\mathbf{k}\sigma} +$$

$$+ \mu \sum_{\mathbf{k},\sigma} \left( c^{+}_{\mathbf{k}\sigma} c_{\mathbf{k}\sigma} + d^{+}_{\mathbf{k}\sigma} d_{\mathbf{k}\sigma} \right) +$$

$$+ \sum_{\mathbf{k}} \Delta_{\mathrm{ev}}(\mathbf{k}) \left( c^{+}_{\mathbf{k}\uparrow} c^{+}_{-\mathbf{k}\downarrow} - d^{+}_{\mathbf{k}\downarrow} d^{+}_{-\mathbf{k}\uparrow} \right) +$$

$$+ \sum_{\mathbf{k}} \Delta_{\mathrm{odd}}(\mathbf{k}) \left( d^{+}_{\mathbf{k}\uparrow} c^{+}_{-\mathbf{k}\downarrow} - c^{+}_{\mathbf{k}\downarrow} d^{+}_{-\mathbf{k}\uparrow} \right) +$$

$$+ 2\frac{N}{V_{\mathrm{attr}}} \sum_{\alpha} |\Delta_{\alpha}|^2, \tag{9}$$

where

$$\Delta_{\mathrm{ev}}(\mathbf{k}) = \sum_{\alpha} \Delta_{\alpha} \cos(\mathbf{k}\boldsymbol{\rho}_{\alpha} - \varphi_{\mathbf{k}}) \tag{10}$$

is the intra-band spin-singlet (even-parity) order parameter, and

$$\Delta_{\mathrm{odd}}(\mathbf{k}) = i \sum_{\alpha} \Delta_{\alpha} \sin(\mathbf{k}\boldsymbol{\rho}_{\alpha} - \varphi_{\mathbf{k}}) \tag{11}$$

is the inter-band spin-singlet (odd-parity) one.

The Bogolyubov transformation in Eq. (9) gives the quasi-particle spectrum (momentum indices on the right-hand side are dropped):

$$E(\mathbf{k}) = \pm\sqrt{\varepsilon^2 + \mu^2 + |\Delta_{\rm ev}|^2 + |\Delta_{\rm odd}|^2 \pm |A|}, \quad (12)$$

where*

$$A^2 = 4\varepsilon^2\mu^2 + 2|\Delta_{\rm odd}|^2\left(2\varepsilon^2 + |\Delta_{\rm ev}|^2\right) +$$
$$+ \Delta_{\rm ev}^2\Delta_{\rm odd}^{*2} + \Delta_{\rm ev}^{*2}\Delta_{\rm odd}^2.$$

When the inter-band pairing is suppressed ($\Delta_{\rm odd} = 0$), the spectrum has familiar Bardeen–Cooper–Schrieffer (BCS) form

$$E(\mathbf{k}) = \pm\sqrt{(\varepsilon \pm \mu)^2 + |\Delta_{\rm ev}|^2}.$$

## 3. Symmetry of the Order Parameters

One can obtain the following finite-temperature equations for the order parameters:

$$\Delta_\alpha = \frac{V_{\rm attr}}{N}\sum_{\mathbf{k},\beta}\Bigg[\cos(\mathbf{k}\boldsymbol{\rho}_\alpha - \varphi_{\mathbf{k}})\cos(\mathbf{k}\boldsymbol{\rho}_\beta - \varphi_{\mathbf{k}}) \times$$
$$\times\left\{\frac{\tanh\frac{\varepsilon(\mathbf{k})+\mu}{2T_c}}{2[\varepsilon(\mathbf{k})+\mu]} + \frac{\tanh\frac{\varepsilon(\mathbf{k})-\mu}{2T_c}}{2[\varepsilon(\mathbf{k})-\mu]}\right\} +$$
$$+ \sin(\mathbf{k}\boldsymbol{\rho}_\alpha - \varphi_{\mathbf{k}})\sin(\mathbf{k}\boldsymbol{\rho}_\beta - \varphi_{\mathbf{k}}) \times$$
$$\times \frac{\sinh\frac{\mu}{T_c}}{2\mu\cosh\frac{\varepsilon(\mathbf{k})+\mu}{2T_c}\cosh\frac{\varepsilon(\mathbf{k})-\mu}{2T_c}}\Bigg]\Delta_\beta, \quad (13)$$

where the first part in the square brackets is the regular BCS term for two bands.

In such a case, Eq. (13) can be written in a matrix form:

$$\frac{1}{V_{\rm attr}}\begin{pmatrix}\Delta_1\\ \Delta_2\\ \Delta_3\end{pmatrix} = \begin{pmatrix}A & B & B\\ B & A & B\\ B & B & A\end{pmatrix}\begin{pmatrix}\Delta_1\\ \Delta_2\\ \Delta_3\end{pmatrix}, \quad (14)$$

where the following notations are used:

$$A = \frac{1}{N}\sum_{\mathbf{k}}\Bigg[\cos^2(\mathbf{k}\boldsymbol{\rho}_\alpha - \varphi_{\mathbf{k}})\left\{\frac{\tanh\frac{\varepsilon(\mathbf{k})+\mu}{2T_c}}{2[\varepsilon(\mathbf{k})+\mu]} + \right.$$
$$\left. + \frac{\tanh\frac{\varepsilon(\mathbf{k})-\mu}{2T_c}}{2[\varepsilon(\mathbf{k})-\mu]}\right\} + \sin^2(\mathbf{k}\boldsymbol{\rho}_\alpha - \varphi_{\mathbf{k}}) \times$$
$$\times \frac{\sinh\frac{\mu}{T_c}}{2\mu\cosh\frac{\varepsilon(\mathbf{k})+\mu}{2T_c}\cosh\frac{\varepsilon(\mathbf{k})-\mu}{2T_c}}\Bigg], \quad (15)$$

$$B = \frac{1}{N}\sum_{\mathbf{k}}\Bigg[\cos(\mathbf{k}\boldsymbol{\rho}_\alpha - \varphi_{\mathbf{k}})\cos(\mathbf{k}\boldsymbol{\rho}_\beta - \varphi_{\mathbf{k}}) \times$$
$$\times\left\{\frac{\tanh\frac{\varepsilon(\mathbf{k})+\mu}{2T_c}}{2[\varepsilon(\mathbf{k})+\mu]} + \frac{\tanh\frac{\varepsilon(\mathbf{k})-\mu}{2T_c}}{2[\varepsilon(\mathbf{k})-\mu]}\right\} +$$
$$+ \sin(\mathbf{k}\rho_\alpha - \varphi_{\mathbf{k}})\sin(\mathbf{k}\boldsymbol{\rho}_\beta - \varphi_{\mathbf{k}}) \times$$
$$\times \frac{\sinh\frac{\mu}{T_c}}{2\mu\cosh\frac{\varepsilon(\mathbf{k})+\mu}{2T_c}\cosh\frac{\varepsilon(\mathbf{k})-\mu}{2T_c}}\Bigg]. \quad (16)$$

In Eq. (15), $\alpha$ has any of three values, and, in Eq. (16), $\alpha$ and $\beta$ are any two different values.

## 4. Main Equations

The eigenvalues of Eq. (14) are

$$\varepsilon_1 = A + 2B - V_{\rm attr}^{-1}, \quad (17)$$
$$\varepsilon_2 = A - B - V_{\rm attr}^{-1}. \quad (18)$$

Now, substitution of eigenvalues (17) and (18) into Eq. (14) gives the eigenvectors, i.e., the order parameter components $\Delta_1 - \Delta_3$, which together with Eq. (13) defining the momentum dependence, and, hence, the symmetry of the order parameter. Below, we consider two solutions in detail.

**1**. From Eq. (17), it can be seen that its solution can be represented in the form

$$\begin{pmatrix}\Delta_1\\ \Delta_2\\ \Delta_3\end{pmatrix} \sim \frac{1}{\sqrt{3}}\begin{pmatrix}1\\ 1\\ 1\end{pmatrix}. \quad (19)$$

This solution and Eq. (10) result in even-parity order parameter

$$\Delta_{\rm ev}(\mathbf{k}) \sim \sum_\alpha \cos(\mathbf{k}\boldsymbol{\rho}_\alpha - \varphi_{\mathbf{k}}). \quad (20)$$

i.e., we have obtained that this order parameter has an ***extended s-symmetry***.

On the other hand, for the inter-band pairing with such a symmetry from Eq. (14) it follows that

$$\Delta_{\rm odd}(\mathbf{k}) = 0. \quad (21)$$

**2**. The solution for (18) is two-fold degenerate and has form

$$\begin{pmatrix}\Delta_1\\ \Delta_2\\ \Delta_3\end{pmatrix} \sim \frac{1}{\sqrt{6}}\begin{pmatrix}2\\ -1\\ -1\end{pmatrix}, \quad \begin{pmatrix}\Delta_1\\ \Delta_2\\ \Delta_3\end{pmatrix} \sim \frac{1}{\sqrt{2}}\begin{pmatrix}0\\ 1\\ -1\end{pmatrix}. \quad (22)$$

Using these results and Eq. (10), one can easily find that

$$\Delta_{\rm ev}\left(\mathbf{k}\right) \sim \begin{cases} 2\cos\left(\mathbf{k}\boldsymbol{\rho}_1 - \varphi_{\mathbf{k}}\right) - \cos\left(\mathbf{k}\boldsymbol{\rho}_2 - \varphi_{\mathbf{k}}\right) - \\ -\cos\left(\mathbf{k}\boldsymbol{\rho}_3 - \varphi_{\mathbf{k}}\right), \\ \cos\left(\mathbf{k}\boldsymbol{\rho}_2 - \varphi_{\mathbf{k}}\right) - \cos\left(\mathbf{k}\boldsymbol{\rho}_3 - \varphi_{\mathbf{k}}\right), \end{cases} \quad (23)$$

or more exactly, this order parameter has an ***extended d-symmetry***.

For the inter-band pairing with extended $s$-symmetry, one gets

$$\Delta_{\rm odd}\left(\mathbf{k}\right) \quad (24)$$

– ***p-symmetry***. It can be simply shown that, in the case of intra-band pairing only, the d-symmetry order parameter appears and is formed at higher critical temperature $T_{\rm c}$. In the following, we consider the case of the intra-band pairing only (i.e., we ignore $\Delta_{\rm odd}\left(\mathbf{k}\right)$), and consider only dominating terms with $\varepsilon\left(\mathbf{k}\right) - \mu$ in Eqs. (15), (16). Such simplifications do not lead to a significant change in the physical results and allow us to analyze the role of the $NNN$ hoping in a transparent way.

For the $s$-wave solution, the value of $T_{\rm c}$ is determined from Eq. (17), which (if we put $\varepsilon_1 = 0$, or when the superconducting gap disappears) has the form

$$1 = V_{\rm attr}\frac{1}{N}\sum_{\mathbf{k}}\left[\cos^2\left(\mathbf{k}\boldsymbol{\rho}_1 - \varphi_{\mathbf{k}}\right) + \right.$$
$$\left. + 2\cos\left(\mathbf{k}\boldsymbol{\rho}_1 - \varphi_{\mathbf{k}}\right)\cos\left(\mathbf{k}\boldsymbol{\rho}_2 - \varphi_{\mathbf{k}}\right)\right]\frac{\tanh\frac{\varepsilon(\mathbf{k})-\mu}{2T_c}}{2\left(\varepsilon\left(\mathbf{k}\right)-\mu\right)}. \quad (25)$$

while in the $d$-wave channel, Eq. (18), it is

$$1 = V_{\rm attr}\frac{1}{N}\sum_{\mathbf{k}}\left[\cos^2\left(\mathbf{k}\boldsymbol{\rho}_1 - \varphi_{\mathbf{k}}\right) - \cos\left(\mathbf{k}\boldsymbol{\rho}_1 - \varphi_{\mathbf{k}}\right)\times\right.$$
$$\left.\times\cos\left(\mathbf{k}\boldsymbol{\rho}_2 - \varphi_{\mathbf{k}}\right)\right]\frac{\tanh\frac{\varepsilon(\mathbf{k})-\mu}{2T_c}}{2\left(\varepsilon\left(\mathbf{k}\right)-\mu\right)} \quad (26)$$

(for definiteness, we used the explicit values for the lattice vector numbers, $\alpha = 1$, $\beta = 2$). Since the main contribution to the sum comes from small momenta, and, for these momenta, $\varphi_{\mathbf{k}}$ is small, to simplify the analysis, we put $\varphi_{\mathbf{k}} = 0$ in the calculations. To account for a possible change in the doping, we solved Eqs. (25) and (26) self-consistently with the particle number equation

$$n_f = \frac{1}{N}\sum_{\mathbf{k}}\left[1 - \tanh\frac{\varepsilon\left(\mathbf{k}\right)-\mu}{2T_c}\right]. \quad (27)$$

## 5. Solutions

Solutions for the critical temperature in both channels as function of the attraction and the ratio $t_{NN}/t_{NNN} = 0.05$ and doping 0.5 are shown in Fig. 3. As it follows from this figure, the $d$-cannel gives a major contribution to superconductivity. This property remains qualitatively the same, as one changes the $NNN$ hopping (Fig. 4). As it follows from Fig. 4, the pairing in the $d$-channel has a few times larger critical temperature. However, the roles of the $NNN$ hopping in both channels are very different. Most notably, at positive values of this hopping, $s$-superconductivity is rapidly suppressed as the hopping increases leading to a pure $d$-pairing at $t_{NNN}$ larger than approximately $0.1t_{NN}$.

One can tune the ratio of the relative contributions of the $s$- and $d$-pairs into the condensate by changing the ratio $t_{NNN}/t_{NN}$, as it follows from Fig. 5. In particular, while the $d$-pairing depends relatively weakly on the $NNN$ hopping, the $s$-channel shows a sharp increase of superconductivity when the $NNN$ hoping approximately satisfies $-0.5t_{NN} < t_{NNN} < 0$. This can be partially explained by modification of the Fermi surface shown in Fig. 2. Namely, the Fermi surface becomes extremely deformed and shifted from K valleys at $t_{NNN}/t_{NN} \sim -0.3$. We also give other arguments on the why this happens in the next Section.

## 6. The Origin of the Opposite Roles of $t_{NNN}$ in $s$- and $d$-Channels

Let us consider two solutions (19) and (23) separately by expanding the critical temperature equations (25)

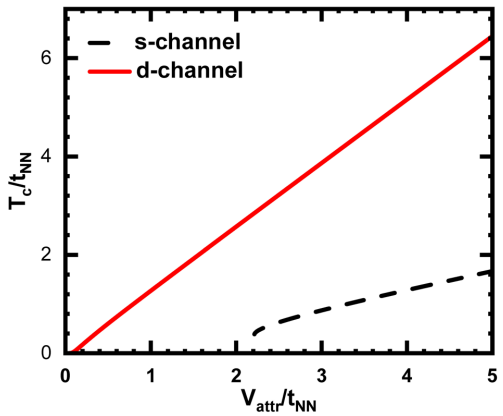


***Fig. 3.*** Critical temperature in different channels as function of the attraction at $t_{NNN} = 0.05t_{NN}$ and a doping of 0.5

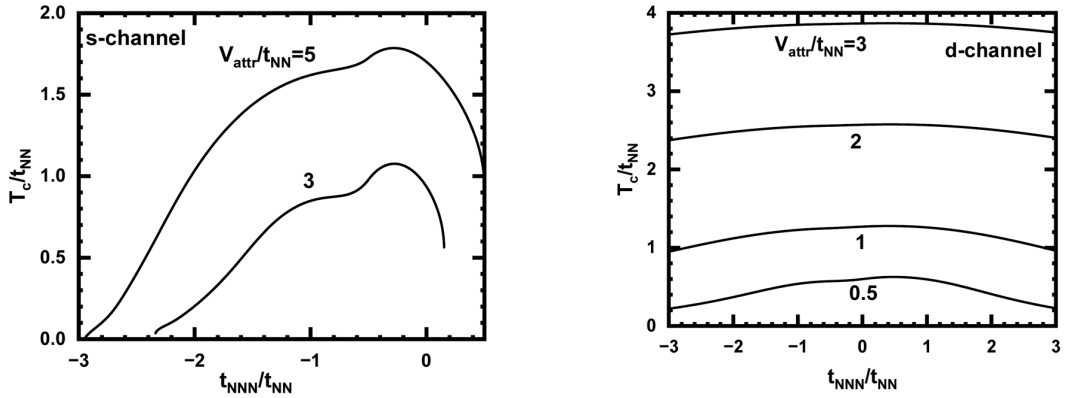


***Fig. 4.*** Critical temperature in different channels as function of the $NNN$ hopping at different values of attraction and a doping of 0.5

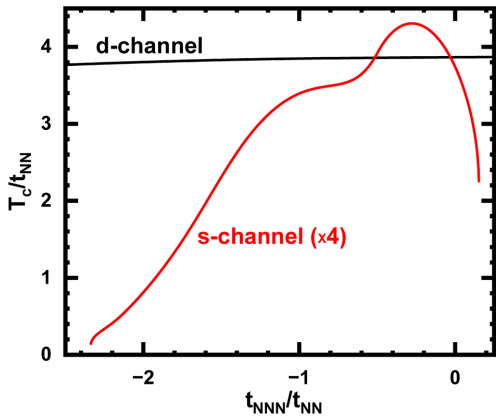


***Fig. 5.*** Critical temperature in the $d$- and $s$- (multiplied by 4) channels as a function of the $NNN$ hopping at $V_{\text{attr}}/t_{NN} = 3$ and a doping of 0.5

and (26) in the linear approximation in $t_{NNN}$. In the s-channel, Eq. (25), for $\mathbf{k}\boldsymbol{\rho}_1 = \frac{1}{2}k_x a + \frac{\sqrt{3}}{2}k_y a$, $\mathbf{k}\boldsymbol{\rho}_2 = \frac{1}{2}k_x a - \frac{\sqrt{3}}{2}k_y a$ gives:

$$1 = V_{\text{attr}}\frac{1}{N}\sum_{\mathbf{k}}\left[2\cos^2\left(\frac{k_x a}{2}\right)\cos^2\left(\frac{k_y\sqrt{3}a}{2}\right) - \right.$$
$$- \frac{1}{2}\sin\left(k_x a\right)\sin\left(k_y\sqrt{3}a\right) -$$
$$\left. - \left(1 - \cos^2\left(\frac{k_x a}{2}\right) - \cos^2\left(\frac{k_y\sqrt{3}a}{2}\right)\right)\right] \times$$
$$\times \frac{\tanh\frac{\varepsilon(\mathbf{k})-\mu}{2T_c}}{2\left(\varepsilon\left(\mathbf{k}\right)-\mu\right)}, \tag{28}$$

while, in the $d$-channel, Eq. (26) transforms into

$$1 = V_{\text{attr}}\frac{1}{N}\sum_{\mathbf{k}}\left[2\cos^2\left(\frac{k_x a}{2}\right)\cos^2\left(\frac{k_y\sqrt{3}a}{2}\right) - \right.$$
$$- \frac{1}{2}\sin\left(k_x a\right)\sin\left(k_y\sqrt{3}a\right) +$$
$$\left. + 2\left(1 - \cos^2\left(\frac{k_x a}{2}\right) - \cos^2\left(\frac{k_y\sqrt{3}a}{2}\right)\right)\right] \times$$
$$\times \frac{\tanh\frac{\varepsilon(\mathbf{k})-\mu}{2T_c}}{2\left(\varepsilon\left(\mathbf{k}\right)-\mu\right)}. \tag{29}$$

Comparison of these two equations shows that the term $\left(1 - \cos^2\left(k_x a/2\right) - \cos^2\left(k_y\sqrt{3}a/2\right)\right)$ in the symmetry factor of the equations has different signs in different channels and is multiplied by 2 in the $d$-channel. Since this term is positive in the $d$-channel, it results in a higher critical temperature. To understand different dependencies of the critical temperature on the $NNN$ hopping, one can expand the remaining (last) factor in Eq. (29) in linear order in $t_{NNN}$. Since $t_{NNN}$ enters the dispersion, let us write down explicit expression for it in the linear order:

$$\varepsilon\left(\mathbf{k}\right) \approx$$
$$\approx 2t_{NN}\sqrt{\cos^2\left(\frac{k_y\sqrt{3}a}{2}\right) + \cos\left(\frac{3k_x a}{2}\right)\cos\left(\frac{\sqrt{3}k_y a}{2}\right)} +$$
$$+ 2t_{NNN}\left[\cos\left(\sqrt{3}k_y a\right) + 2\cos\left(\frac{3k_x a}{2}\right)\cos\left(\frac{\sqrt{3}k_y a}{2}\right)\right]. \tag{30}$$

The last term has the following momentum dependence at small momenta:

$$2t_{NNN}\left[3 - \frac{9}{4}\left(\left(k_x a\right)^2 + \left(k_y a\right)^2\right)\right] \approx 6t_{NNN}.$$

Thus, the multiplication of such a term by different factors in different channels

$$-\left(1-\cos^2\left(k_x a/2\right)-\cos^2\left(k_y\sqrt{3}a/2\right)\right)$$

and

$$2\left(1-\cos^2\left(k_x a/2\right)-\cos^2\left(k_y\sqrt{3}a/2\right)\right),$$

leads to different contributions of the $NNN$ to the superconducting pairing (basically, modifying the symmetry of the pairing).

## 7. Summary

We have analyzed the role of the $NNN$ hopping on the superconducting properties of the honeycomb-lattice model with $NN$ attraction. It is found that the $d$-channel gives a major contribution to the superconducting condensate at any value of $t_{NNN}$, while, at $-0.5t_{NN} < t_{NNN} < 0$, there is a significant contribution from the $s$-channel. The rapid decrease of superconductivity with the growth of $t_{NNN}$ needs to be studied in more details. Naturally, it is not possible to tune separately the $NNN$ component of the hopping matrix, and we just explored the role of this part of the hopping in the superconducting properties of the system with a honeycomb lattice (e.g., in graphene and 2D transition metal dichalcogenides).

As we mentioned above, the role of the $NNN$ carrier hoping in the superconductivity of 2D systems is barely analyzed. However, besides the obvious case of the electronic spectrum, this parameter defines the attraction between the electrons, or, more accurately, it makes this attraction different in different channels, when the pairs are formed on $NN$ sites (nematic superconductivity). The last effect is, to some extent, an unexpected result of this work. We also would like to note that the effect can be especially relevant to cuprate high-temperature superconductors with a different, square-type, lattice. Though this problem requires a separate quantitative/numerical study, even without such an analysis, it is obvious that, in cuprates, a competition between the $s$- and $d$-wave channels may come from a nonzero $t_{NNN}$ only. Besides, an important problem, overlooked by theorists and experimentalists so far, is crossover from (actually local) nematic pairs to large Cooper pairs with doping increasing. The study above is the first step toward solving these interesting and important problems.

*The work of V.L. was partially supported by Grants No. 0117U000236 and No. 0117U000240 from the National Academy of Sciences of Ukraine, and also he had the partial support from the Simons Foundation (USA). The work of V.T. was supported in part by United States Department of Energy under grant No. DE-FG02-07ER46354.*

1. B. Uchoa, G.G. Cabrera, A.H. Castro Neto. Nodal liquid and $s$-wave superconductivity in transition metal dichalcogenides. *Phys. Rev. B* **71**, 184509 (2005).
2. B. Uchoa, A.H. Castro Neto. Superconducting states of pure and doped graphene. *Phys. Rev. Lett.* **98**, 146801 (2007).
3. E. Zhao, A. Paramekanti. BCS-BEC crossover on the two-dimensional honeycomb lattice. *Phys. Rev. Lett.* **97**, 230404 (2006).
4. V.M. Loktev, V. Turkowski. Suppression of the superconducting transition temperature of doped graphene due to thermal fluctuations of the order parameter. *Phys. Rev. B* **79**, 233402 (2009).
5. G. Savini, A.C. Ferrari, F. Giustino. First-principles prediction of doped graphane as a high-temperature electron-phonon superconductor. *Phys. Rev. Lett.* **105**, 037002 (2010).
6. V.M. Loktev, V. Turkowski. Possible high-temperature superconductivity in multilayer graphane: Can the cuprates be beaten? *J. Low Temp. Phys.* **164**, 264 (2011).
7. M. Black-Schaffer, C. Honerkamp. Chiral $d$-wave superconductivity in doped graphene. *J. Phys.: Condens. Matter* **26**, 423201 (2014).
8. E.R. Margine, F. Giustino. Two-gap superconductivity in heavily-doped graphene: Ab initio Migdal-Eliashberg theory. *Phys. Rev. B* **90**, 014518 (2014).
9. A. García-Ruiz, M. Mucha-Kruczyński, V.I. Fal'ko. Superconductivity-induced features in the electronic Raman spectrum of monolayer graphene. *Phys. Rev. B* **97**, 155405 (2018).
10. R.T. Tagiyeva Askerbeyli, I.N. Askerzade. BCS superconductivity of Dirac electrons in graphene monolayer. *J. Supercond. Novel Magnet.* **32**, 1871 (2019).
11. E. Thingstad, A. Kamra, J.W. Wells, A. Sudbø. Phonon-mediated superconductivity in doped monolayer materials. *Phys. Rev. B* **101**, 214513 (2020).
12. A.L. Szabó, B. Roy. Extended Hubbard model in undoped and doped monolayer and bilayer graphene: Selection rules and organizing principle among competing orders. *Phys. Rev. B* **103**, 205135 (2021).
13. D. Qiu, C. Gong, S.S. Wang, M. Zhang, C. Yang, X. Wang, J. Xiong. Recent advances in 2D superconductors. *Adv. Mater.* **33**, 2006124 (2021).
14. A.M. Black-Schaffer, K. Le Hur. Topological superconductivity in two dimensions with mixed chirality. *Phys. Rev. B* **92**, 140503(R) (2015).

15. J.P.L. Faye, P. Sahebsara, D. Senechal. Chiral triplet superconductivity on the graphene lattice. *Phys. Rev. B* **92**, 085121 (2015).
16. J. Yuan, C. Honerkamp. Triplet pairing driven by Hund's coupling in doped monolayer $MoS_2$. *Preprint arXiv: 1504.04536v2* (2015).
17. D.-H. Lee, C.-H. Chung. Non-centrosymmetric superconductors on honeycomb lattice. *Phys. Status Solidi B* **255**, 1800114 (2018).
18. Y.F. Suprunenko, E.V. Gorbar, V.M. Loktev, S.G. Sharapov. Effect of next-nearest-neighbor hopping on the electronic properties of graphene. *Low Temp. Phys.* **34**, 812 (2008).
19. T. Farajollahpour, A.H. Rezvani, M.R. Khodarahmi, M. Arasteh. Next nearest neighbors effects on berry curvature of graphene. *Acta Phys. Polonica A* **122**, 180 (2012).
20. L.-Y. Xiao, S.-L. Yu, W. Wang, Z.-J. Yao, J.-X. Li. Possible singlet and triplet superconductivity on honeycomb lattice. *Eur. Phys. Lett.* **115**, 27008 (2016).
21. X. Zhu, T. Ying, H. Guo, S. Feng. Quantum Monte Carlo study of the dominating pairing symmetry in doped honeycomb lattice. *Chin. Phys. B* **28**, 077401 (2019).
22. L. Classen, A.V. Chubukov, C. Honerkamp, M.M. Scherer. Competing orders at higher-order Van Hove points. *Phys. Rev. B* **102**, 125141 (2020).
23. P. Jia, S. Yang, W. Li, J. Yang, T. Ying, X. Li, X. Sun. Pairing in the Hubbard model on the honeycomb lattice with hopping up to the third-nearest-neighbor. *Phys. Lett. A* **442**, 128175 (2022).
24. X.-D. Li, H.-R. Liu, Z.-D. Yu, C.-D. Gong, S.-L. Yu, Y. Zhou. Mixture of the nearest- and next-nearest-neighbor $d + id$-wave pairings on the honeycomb lattice. *New J. Phys.* **24**, 103035 (2022).
25. J. Wang, X. Zhang, R. Ma, G. Yang, E.V. Castro, T. Ma. Spin-triplet superconducting pairing in doped $MoS_2$. *Phys. Rev. B* **106**, 134513 (2022).
26. X. Han, A.P. Schnyder, X. Wu. Enhanced nematicity emerging from higher-order Van Hove singularities. *Phys. Rev. B* **107**, 184504 (2023).
27. L. Fu. Odd-parity topological superconductor with nematic order: Application to $Cu_xBi_2Se_3$. *Phys. Rev. B* **90**, 100509(R) (2014).
28. S. Yonezawa, K. Tajiri, S. Nakata, Y. Nagai, Z. Wang, K. Segawa, Y. Ando, Y. Maeno. Thermodynamic evidence for nematic superconductivity in $Cu_xBi_2Se_3$. *Nature Phys.* **13**, 123 (2017).
29. S. Wolf, D. Di Sante, T. Schwemmer, R. Thomale, S. Rachel. Triplet superconductivity from nonlocal Coulomb repulsion in an atomic Sn layer deposited onto a Si(111) substrate. *Phys. Rev. Lett.* **128**, 167002 (2022).
30. P. Rosenzweig, H. Karakachian, D. Marchenko, K. Küster, U. Starke. Overdoping graphene beyond the van Hove singularity. *Phys. Rev. Lett.* **125**, 176403 (2020).

Received 16.06.24

*В.М. Локтев, В. Турковський*

СИМЕТРІЯ ТА ЗНАЧЕННЯ
ПАРАМЕТРА ПОРЯДКУ У ДВОВИМІРНИХ
НЕМАТИЧНИХ НАДПРОВІДНИКАХ

У цій роботі ми вивели рівняння для надпровідного нематичного параметра порядку та хімічного потенціалу для гексагональної ґратки з урахуванням перескоку електронів на найближчі і наступні після найближчих вузли. З аналізу енергії основного надпровідного стану було встановлено, що симетрія параметра порядку та деякі інші надпровідні властивості системи сильно залежать від знака та модуля параметра перескоку на наступні після найближчих вузли. Як показано, спарювання з розширеною $s$- і $d$-симетрією дають значний внесок у надпровідне спарювання в системі, яке можна змінювати, варіюючи параметри перескоку. Обговорено можливий зв'язок отриманих результатів із властивостями деяких одношарових допованих надпровідників (графену і дихалькогенідів перехідних металів).

*Ключові слова:* теорія надпровідності, 2D системи, нематичність.